J Mol Model (2014) 20:2524
DOI 10.1007/s00894-014-2524-x

ORIGINAL PAPER

An interpretation of the phenol nitration mechanism in the gas phase using G3(MP2)//B3-CEP theory

Carlos Murilo Romero Rocha · José Augusto Rosário Rodrigues · Paulo José Samenho Moran · Rogério Custodio

Received: 22 August 2014 / Accepted: 7 November 2014 / Published online: 30 November 2014

Abstract G3(MP2)//B3-CEP theory was applied to study the mechanism of phenol nitration in the gas phase, as promoted by the electrophile NO_2^+. The results of studying this mechanism at the G3(MP2)//B3-CEP level pointed to the occurrence of a single-electron transfer (SET) from the aromatic π-system to the nitronium ion prior to σ-complex formation. The formation of an initial π-complex between the nitronium ion and phenol was not observed. Excellent agreement between the activation barriers predicted by G3(MP2)//B3-CEP and those yielded by other, more accurate, versions of the G3 theory showed that the former is a useful tool for studying reaction mechanisms, as G3(MP2)//B3-CEP is much less computationally expensive than other high-level methods.

Keywords Phenol nitration · Electrophilic aromatic substitution · G3(MP2)//B3-CEP theory · Single electron transfer

Electronic supplementary material The online version of this article (doi:10.1007/s00894-014-2524-x) contains supplementary material, which is available to authorized users.

C. M. R. Rocha · J. A. R. Rodrigues · P. J. S. Moran · R. Custodio (✉)
Instituto de Química, Universidade Estadual de Campinas, Barão Geraldo, 13083-970 Campinas, São Paulo, BrazilP.O. Box 6154
e-mail: roger@iqm.unicamp.br

Present Address:
C. M. R. Rocha
Departamento de Química, Universidade de Coimbra, 3004-535 Coimbra, Portugal

Introduction

Electrophilic aromatic substitution reactions are widely studied in organic chemistry, both experimentally and theoretically [1, 2]. Among such reactions, electrophilic aromatic nitration stands out because studies of its mechanism provide key insights into the reactivity and selectivity of aryl compounds, allowing further development of the basic principles of physical organic chemistry [1–3].

Hughes and Ingold proposed the classical mechanism of aromatic nitration [4], in which the nitronium ion (NO_2^+) plays an essential role as a reactive electrophile in the reaction medium. As shown in Fig. 1, in the presence of a strong acid (typically sulfuric acid), nitric acid (HNO_3) generates the NO_2^+ ion. Subsequently, in the rate-determining step of the mechanism, the nitronium ion reacts with the aromatic compound, resulting in a Wheland intermediate, which is also known as an arenium ion and commonly referred to as a σ-complex [5]. This intermediate undergoes rapid deprotonation (promoted by a Lewis base, B:), providing the nitrated product.

The formation and stability of the σ-complex explain the effects of positional orientation observed in nitration reactions. For example, the presence of σ- and π-electron-donating side groups (R) stabilizes the arenium ion formed, producing nitrated products in the *ortho* and *para* positions with respect to the R group. In contrast, π- and/or σ-electron-accepting side groups (R) destabilize the arenium ion formed in the *ortho* and *para* positions with respect to the R group, resulting in the product being nitrated in the *meta* position [1–3]. Moreover, differences in the reactivities and therefore the velocities of nitration of monosubstituted aromatic substrates can be attributed to the various donating or accepting effects of substituent groups on the ring in the Ingold–Hughes mechanism.

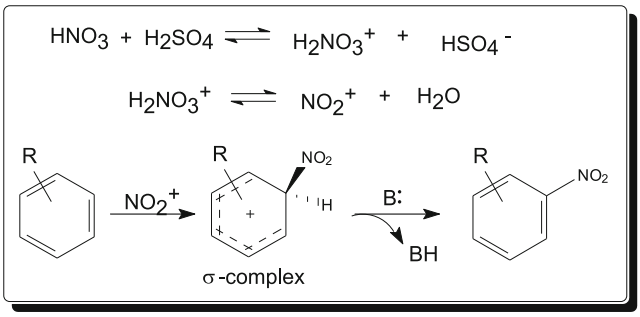

Fig. 1 The Ingold–Hughes mechanism

Modifications to the classical Ingold–Hughes mechanism have been proposed by Olah et al. [6]. They suggested the existence of an additional intermediate that precedes the step in which the σ-complex is obtained, as shown in Fig. 2. The proposed intermediate was considered a Dewar-type complex [7], or a π-complex [8], with an electrophile (NO_2^+) that interacts weakly and nonspecifically with the rest of the aromatic π-system. Olah proposed that, for activated substrates, the rate-determining step is the formation of a π-complex. However, for deactivated substrates, when π- and/or σ-electron-accepting substituents are present, a σ-complex determines the reaction rate.

Kenner [9] and Weiss [10] have also suggested the existence of alternative reaction pathways through which single-electron transfer steps would be observed. This mechanism was later confirmed by Perrin [11] and Kochi [12]. As illustrated in Fig. 3, the single-electron transfer (SET) mechanism consists of the initial formation of a charge-transfer complex (CTC) or a π-type complex [13] that is converted to the SET intimate pair after a phase of single-electron transfer. Subsequently, combination of the aromatic radical cation and the NO_2 radical results in a σ-complex, from which the nitrated product is obtained. Therefore, as proposed by Kochi [12], the rate-determining step for the reaction is the formation of the SET inner pair.

In addition to experimental observations performed in the condensed phase, theoretical studies [14–23] investigating the mechanism for the electrophilic nitration of benzene and monosubstituted derivatives in the gas phase have elucidated important details that support the existence of single-electron transfer steps.

Queiroz et al. [17], based on theoretical calculations carried out at the B3LYP/6-311++G(d, p) level as well as mass spectrometric studies, presented an alternative model for the electrophilic aromatic nitration reaction. The model consists of a continuous mechanism in which the nature of the substituent on the aromatic compound determines the preferred reaction path according to the model of Ingold–Hughes, Olah, or SET. Thus, for the nitration of substrates containing *ortho/para*-directing groups, the reaction converges to the SET mechanism, whereas for the nitration of substrates containing *meta*-directing groups, the classical Ingold–Hughes mechanism and/or the Olah path will be observed. It is worth noting that the preference for a specific reaction path is significantly influenced by solvent and counterion effects [16, 17, 24–26]. Mass spectrometric studies of ion–molecule reactions in the gas phase show that the reaction of the NO_2^+ ion with benzene does not lead to the formation of nitrated products, but rather $C_6H_6O^+$, which results from O^+ transfer to the aromatic ring [24]. Theoretical studies performed by Esteves et al. [16] of benzene in the presence of the nitronium ion have supported this observation. The results showed that, in the gas phase, species derived from the transfer of O^+ to the benzene ring were more stable, even when compared with the corresponding nitro compounds.

However, Ashi et al. [25] demonstrated that when ion–molecule reactions are carried out in the gas phase using nitronium ion carrier species such as $[CH_3OH–NO_2]^+$, the products obtained arise from the direct nitration of the aromatic compound, and the observed positional selectivity is similar to that seen in condensed-phase studies.

Despite the large number of papers in the literature that focus on studies of electrophilic aromatic nitration [1–26], there are still important aspects of this process that need to be explained [17]. Whereas experimental data show the existence of several reaction pathways [3, 13, 24–26], theoretical studies based on less accurate methods consider single electron transfer (SET) to be the most plausible explanation for the nitration reactions of substrates containing *ortho/para* directors [14–23].

The purpose of the work reported in the present paper was therefore to perform a theoretical study of the nitration mechanism of phenol in the gas phase using a new formulation of G3(MP2)//B3 theory that includes a pseudopotential, referred to as G3(MP2)//B3-CEP theory [27]. The aim was to assess the relevant aspects of the intermediates formed in the reaction process.

Computational methods

The G3 theory [28] and computationally less expensive versions of it, such as G3(MP2) [29] and G3(MP2)//B3 [30], are

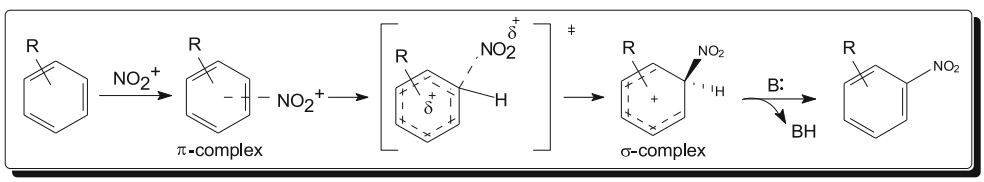

Fig. 2 Modified mechanism proposed by Olah

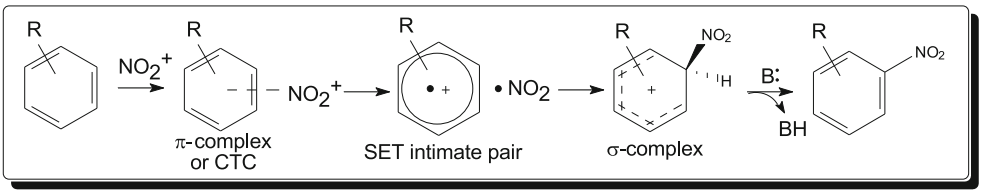

Fig. 3 Single-electron transfer (SET) mechanism

quantum mechanical methods that have been widely used in the study of a variety of compounds [31–34], rotational barriers [35, 36], and mechanisms [37–39]. However, the size of molecular systems continues to be a limiting factor that prevents the more general use of Gaussian-n theories.

Recently, the compact effective pseudopotential (CEP) developed by Steve, Basch, and Krauss [40, 41] was implemented in G3 [28] and G3(MP2)//B3 [30]; the resulting methods are referred to as G3CEP [42, 43] and G3(MP2)//B3-CEP [27], respectively. These methods were tested against the G3/05 test set [44] and produced similar results to those provided by the original methods, yielding similar mean absolute deviations, but with a substantial reduction in the CPU time.

The G3(MP2)//B3-CEP theory [27] is derived from a set of ab initio calculations with an energy ($E_{G3(MP2)//B3\text{-}CEP}$) that approximates the energy obtained by a calculation performed at the *E*[QCISD(T,Frz)/CEP-G3MP2large] level of theory, according to the following expression:

$$E_{G3(MP2)//B3-CEP} = E[\mathrm{QCISD(T,\,Frz)/CEP{-}P31G(d)}] + \Delta E_{CEP-G3MP2large} + \Delta E_{HLC} + E_{SO} + E_{ZPE}, \quad (1)$$

where the *E*[QCISD(T,Frz)/CEP-P31G(d)] energy term is improved by including the following corrections: (a) $\Delta E_{CEP\text{-}G3MP2large} = E[\mathrm{MP2/CEP\text{-}}G3\mathrm{MP2large}] - E[\mathrm{MP2/CEP\text{-}P31}G\mathrm{(d)}]$; (b) the spin-orbit correction taken from atomic experimental measurements and theoretical calculations, E_{SO}; (c) the zero-point energy and vibrational corrections, E_{ZPE}; and (d) a higher-level correction (HLC) to account for residual electronic and basis set effects. The last correction is expressed as $\Delta E_{HLC} = -A.n_\beta - B.(n_\alpha - n_\beta)$ for molecules and $\Delta E_{HLC} = -C.n_\beta - D.(n_\alpha - n_\beta)$ for atoms, where n_α and n_β are the number of valence electrons with alpha and beta spins, respectively, $n_\alpha \geq n_\beta$, and *A*, *B*, *C*, and *D* are parameters that are optimized to give the smallest mean absolute deviation from the experimental data. All of the steps required and HLC parameters used to calculate the G3(MP2)//B3-CEP energy are described in the literature [27].

For elementary steps in which transition states were observed, intrinsic reaction coordinate [45] calculations were performed at the B3LYP/CEP-P31G(d) level to determine the minimum energy path interconnecting transition states and the associated minima of reactants and products. From the equilibrium and transition geometries, the ground and transition-state energies were calculated at the $E_{G3(MP2)//B3\text{-}CEP}$ level of theory. Several initial random structures were considered in the determination of the optimum equilibrium and transition structures. The procedure is not a fully stochastic method as described in the literature [46], but the potential energy surface was explored thoroughly. The charge distributions were obtained at the *E*[QCISD(T,Frz)/CEP-P31G(d)] level and calculated from natural population analysis (NPA) [47, 48]. All of the calculations were carried out with the Gaussian 09 program [49].

Results and discussion

The mechanism for the nitration of phenol using the nitronium ion (NO_2^+) as the electrophile was studied. The Gibbs free energies of the reactants, products, and transition states obtained at the G3(MP2)//B3-CEP level in the gas state at a temperature of 298.15 K are shown in Fig. 4. The geometric parameters of the optimized structures calculated at the B3LYP/CEP-P31G(d) level and their G3(MP2)//B3-CEP energies are listed in Table S1 of the "Electronic supplementary material" (ESM). The proposed mechanism for the title reaction along with the corresponding structures are summarized in Fig. 5.

As shown in Figs. 4 and 5, the approach of the nitronium ion to the aromatic π-system of phenol leads directly to the

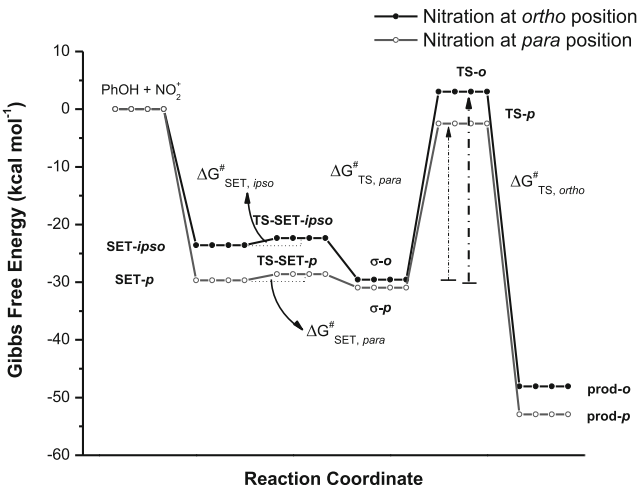

Fig. 4 Gibbs free energy diagram for phenol nitration in the gas phase at a temperature of 298.15 K

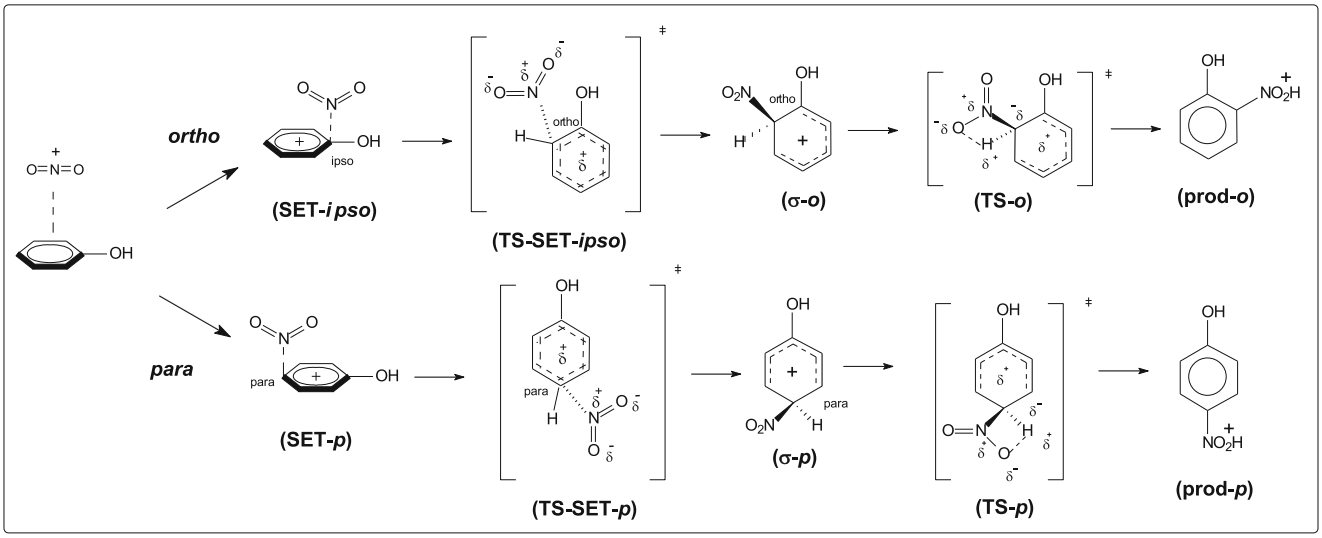

Fig. 5 Proposed mechanism that leads to *ortho*- and *para*-nitrated products

formation of SET-*ipso* and SET-*p* intermediates with relative stabilizations of −23.58 and −29.68 kcal mol^{-1}, respectively. In other words, the intermediates are not obtained via the initial π-complex. In addition, both reaction paths suggest that the formation of the initial intermediate occurs without activation barriers. The structures in Fig. 6 show pronounced distortion of the O–N–O bond angle from 180° in the case of an isolated nitronium ion to 139.9° and 130.7° for the SET-*ipso* and SET-*p* compounds, respectively. The similarity of these angles to the bond angle of NO_2 (134.1°) has been stressed in the literature [50]. This behavior differs from the nitration of benzene, which may involve stable intermediates formed via the π-orbitals [51] in the absence of *ortho*/*para*-directing groups. It is worth remembering that the geometry search is carried out at the B3LYP/CEP-P31G(d) level of theory in the composite method used in this work, which means that we cannot rule out the possibility of a π-intermediate occurring at a much higher level of theory.

To investigate the nature of the SET-*p* and SET-*ipso* structures, NPA charges [47] were obtained for NO_2 and the phenol fragments for each intermediate. The results are shown in Table 1. The results of the NPA analysis indicate that, for both structures, the positive charge is almost entirely localized on the aromatic ring (SET-*ipso*=0.820 and SET-*p*=0.982), and its magnitude is clearly dependent on the distance between NO_2 and the phenol fragments. These results, combined with the distortions to the angle O–N–O, demonstrate the occurrence of a single-electron transfer from the aromatic π-system to the nitronium ion during steps that precede the formation of the σ-complex, as proposed for the SET mechanism [12, 16, 17].

The conversion from SET-*ipso* and SET-*p* to σ-*o* and σ-*p* intermediates (Fig. 8) occurs via the respective TS-SET-*ipso* and TS-SET-*p* transition states, shown in Figs. 5 and 7. These species were characterized by calculating harmonic vibrational frequencies, and they exhibited the presence of only one imaginary frequency each for TS-SET-*ipso* and TS-SET-*p* (117.02*i* cm^{-1} and 26.73*i* cm^{-1}, respectively).

As shown in Fig. 7 and in the ESM, the displacement vectors of the imaginary normal modes of vibration show the arrangement of the NO_2 fragment during the formation of the N–C_{ortho} and N–C_{para} bonds. The activation energies

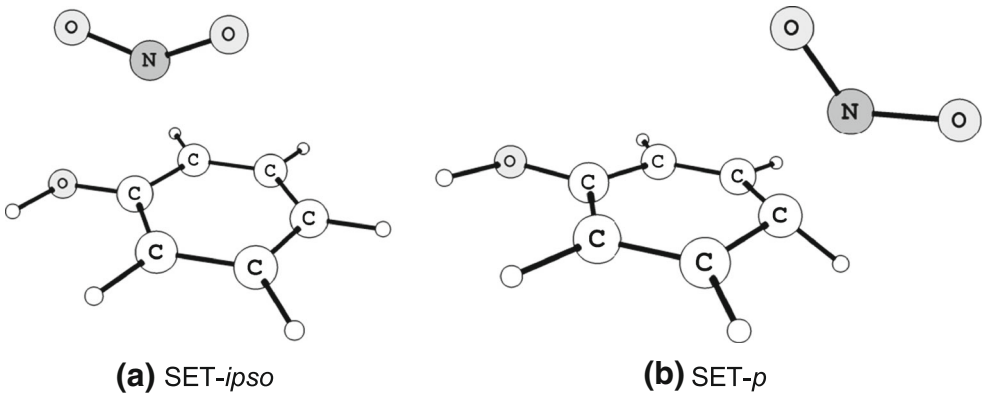

Fig. 6 Structures of the initial intermediates

Table 1 NPA charges obtained for NO_2 and phenol in the SET-*ipso* and SET-*p* intermediates. Distances (*d*) between the fragments are in Å

	$Q_{NPA}(NO_2)$	$Q_{NPA}(C_6H_5OH)$	$d(NO_2–C_6H_5OH)$
SET-*ipso*	0.180	0.820	2.24
SET-*p*	0.017	0.982	1.68

required to obtain the TS-SET-*ipso* and TS-SET-*p* transition states are 1.22 kcal mol^{-1} and 1.09 kcal mol^{-1}, respectively (see Fig. 4 and Table 2). If the G3(MP2)//B3-CEP energies at 298.15 K are used, these barriers change to 0.82 kcal mol^{-1} and 0.58 kcal mol^{-1}, respectively (see results in parentheses in Table 2). These barrier heights were also calculated at the G3(MP2)B3 [30], G3CEP [42, 43], and G3 [28] levels, and the results are shown in Table 2. While the activation energies are small, these steps show the correct interconversion from the SET-*ipso* and SET-*p* intermediates to the respective σ-complexes, and therefore likely correspond to quick steps in the reaction mechanism.

Figures 5 and 8 show that the σ-*o* and σ-*p* intermediates are obtained from a complete two-electron transfer (or polar addition) between the aromatic π-system and the nitronium ion. Large relative stabilizations of −30.96 kcal mol^{-1} and −29.54 kcal mol^{-1} were observed for σ-*p* and σ-*o*, respectively (see Fig. 4), based on either the Gibbs free energy or the G3(MP2)//B3-CEP energy thermally corrected at 298.15 K (−40.47 kcal mol^{-1} and −39.78 kcal mol^{-1}, respectively). It is worth mentioning that the substituted arenium ion at the *meta* position relative to the phenolic hydroxyl was not observed in the present study, reinforcing the strong *ortho/para*-directing character of the hydroxyl group.

The SET-*p* and σ-*p* intermediates are more stable than the respective SET-*ipso* and σ-*o* intermediates, as shown in Fig. 4.

Table 2 Gibbs free activation barriers, $\Delta G_{SET,ipso}$ and $\Delta G_{SET,para}$, calculated at the G3(MP2)//B3-CEP, G3(MP2)B3, G3CEP, and G3 levels of theory. The respective energies calculated excluding the entropic contribution are shown in parentheses

	ΔG_{SET} (kcal mol^{-1} 298.15 K)			
	G3(MP2)//B3-CEP	G3(MP2)B3	G3CEP	G3
$\Delta G_{SET,ipso}$	1.22 (0.82)	1.14 (0.72)	1.78 (0.98)	1.53 (0.58)
$\Delta G_{SET,para}$	1.09 (0.58)	0.99 (0.55)	0.67 (0.30)	0.76 (0.45)

The considerable stabilization of the SET-*p* species with respect to SET-*ipso* (6.10 kcal mol^{-1}) reflects the greater proximity of NO_2 to the aromatic ring (1.68 Å for SET-*p*), as shown in Table 1.

Conversion of the σ-*o* and σ-*p* intermediates to the prod-*o* and prod-*p* protonated products occurs through the respective TS-*o* and TS-*p* transition states shown in Figs. 5 and 9. Such species were characterized by the presence of only one imaginary frequency, with calculated values of 1764.32i cm^{-1} for TS-*o* and 1739.36i cm^{-1} for TS-*p*. As shown in Fig. 9, these imaginary frequencies correspond to the cleavage of C_{ortho}–H and C_{para}–H bonds, respectively, followed by ONO–H bond formation.

The potential energy surface in this study was employed without the presence of Lewis bases and/or nitronium ion carriers. Therefore, as seen in the TS-*o* and TS-*p* structures, deprotonation of the σ-*o* and σ-*p* intermediates occurs through isomerization steps promoted by oxygen atoms of the respective nitro groups. Table 3 shows the Gibbs free activation barriers calculated using the G3(MP2)//B3-CEP, G3(MP2)B3, G3CEP, and G3 theories as well as the barriers calculated at these levels of theory without entropic correction

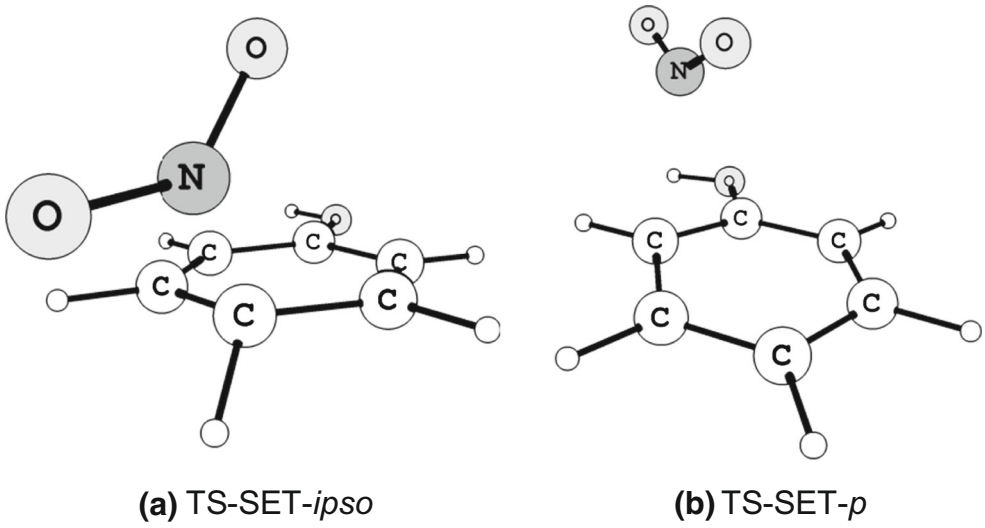

(a) TS-SET-*ipso* **(b)** TS-SET-*p*

Fig. 7 Transition-state structures of TS-SET-*ipso* and TS-SET-*p*

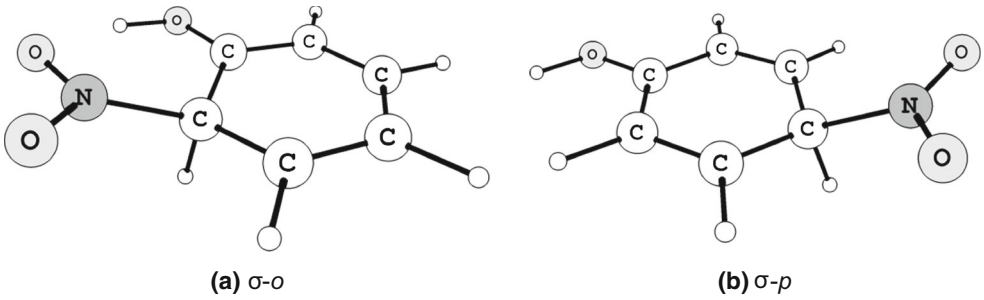

Fig. 8 Structures of the σ-complexes

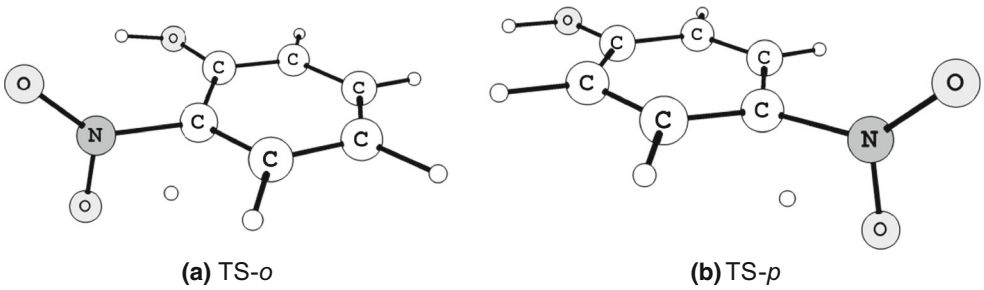

Fig. 9 Transition-state structures of TS-*o* and TS-*p*

Table 3 Gibbs free activation barriers, $\Delta G_{TS,ortho}$ and $\Delta G_{TS,para}$, calculated at the G3(MP2)//B3-CEP, G3(MP2)B3, G3CEP, and G3 levels of theory. The respective energies calculated excluding the entropic contribution are shown in parentheses

	ΔG_{TS} (kcal mol^{-1} 298.15 K)			
	G3(MP2)//B3-CEP	G3(MP2)B3	G3CEP	G3
$\Delta G_{TS,ortho}$	32.59 (33.12)	32.51 (33.04)	32.73 (33.29)	32.52 (33.29)
$\Delta G_{TS,para}$	28.46 (27.97)	28.50 (27.82)	28.91 (28.09)	28.62 (28.06)

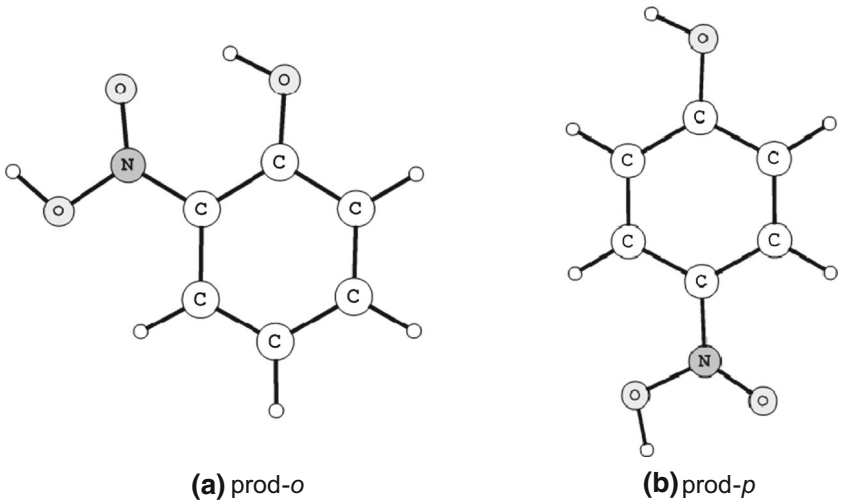

Fig. 10 Structures of the products

(data in parentheses). The activation barriers to the formation of prod-*o* are approximately 4 kcal mol^{-1} higher than those obtained for the formation of prod-*p*. The excellent agreement between the results of G3(MP2)//B3-CEP theory and those of the other more computationally expensive composite methods, G3(MP2)B3, G3CEP, and G3, also demonstrates the accuracy of the G3(MP2)//B3-CEP method in the calculation of activation barriers with reduced computational cost.

This mechanistic study demonstrates the high stability of nitrated products compared to the reactants, i.e., −48.05 kcal mol^{-1} for prod-*o* and −52.91 kcal mol^{-1} for prod-*p* (Figs. 4 and 10). Here, prod-*p* is the protonated product derived from nitration at the *para* position; it is 4.85 kcal mol^{-1} more stable and has a lower activation barrier than the respective *ortho*-substituted product (prod-*o*).

Nevertheless, G3(MP2)//B3-CEP calculations carried out for deprotonated prod-*o* and prod-*p* showed an inversion of the relative stabilities of the compounds, i.e., the *o*-nitrophenol is 1.76 kcal mol^{-1} more stable than *p*-nitrophenol. The same tendency is observed in experimental studies in the condensed phase, which show a moderate preference for the *o*-nitro isomer as the reaction product [52].

Conclusions

G3(MP2)//B3-CEP theory was applied to study the reaction mechanism of the gas-phase nitration of phenol promoted by the electrophile NO_2^+. The formation of the initial π-complex, as proposed by Olah et al. [6], between the nitronium ion and phenol was not observed. However, direct observation of the SET-*ipso* and SET-*p* intermediates and an investigation of their characteristics confirmed the contribution of a single electron transfer from the aromatic π-system of phenol to the nitronium ion during the steps preceding the formation of the σ-complex, as proposed by Kochi [12] and as observed by Queiroz [17] and Esteves [16]. Therefore, our results are consistent with the SET mechanism hypothesis.

The excellent agreement between the results afforded by G3(MP2)//B3-CEP theory and those yielded by the most accurate Gn methods, such as G3(MP2)B3, G3CEP, and G3, demonstrate the utility of the former for predicting accurate activation barriers while significantly reducing the computational cost.

Acknowledgments We acknowledge financial support from FAPESP (Fundação de Amparo à Pesquisa do Estado de São Paulo—Center for Computational Engineering and Sciences, grant 2013/08293-7), CNPq (Conselho Nacional de Desenvolvimento Científico e Tecnológico), and FAEPEX-UNICAMP (Fundo de Apoio ao Ensino, à Pesquisa e à Extensão da UNICAMP). The National Center of High Performance Computing in São Paulo (CENAPAD–SP) is acknowledged for making its computational facilities available to us.

References

1. Taylor R (1990) Electrophilic aromatic substitution, 1st edn. Wiley, Chichester
2. Cardoso SP, de Carneiro JWM (2001) Nitração aromática: substituição eletrofílica ou reação com transferência de elétrons? Quim Nova 24:381–389. doi:10.1590/S0100-40422001000300015
3. Olah GA, Malhotra R, Narang SC (1989) Nitration. Methods and mechanisms. VCH, Weinheim
4. Hughes ED, Ingold CK, Reed RI (1950) Kinetics and mechanism of aromatic nitration. Part II. Nitration by the nitronium ion, NO_2^+, derived from nitric acid. J Chem Soc. doi:10.1039/jr9500002400
5. Wheland GW (1942) A quantum mechanical investigation of the orientation of substituents in aromatic molecules. J Am Chem Soc 64:900–908. doi:10.1021/ja01256a047
6. Olah GA, Kuhn SJ, Flood SH (1961) Aromatic substitution. VIII. Mechanism of the nitronium tetrafluoroborate nitration of alkylbenzenes in tetramethylene sulfone solution. Remarks on certain aspects of electrophilic aromatic substitution. J Am Chem Soc 83: 4571–4580. doi:10.1021/ja01483a017
7. Dewar MJS (1946) The kinetics of some benzidine rearrangements, and a note on the mechanism of aromatic substitution. J Chem Soc 777–781. doi:10.1039/jr9460000777
8. Olah GA (1971) Aromatic substitution. XXVIII. Mechanism of electrophilic aromatic substitutions. Acc Chem Res 4:240–248. doi: 10.1021/ar50043a002
9. Kenner J (1946) Oxidation and reduction in chemistry. Nature 157: 340–340. doi:10.1038/157340a0
10. Weiss J (1946) Simple electron transfer processes in systems of conjugated double bonds. Trans Faraday Soc 42:116. doi:10.1039/tf9464200116
11. Perrin CL (1977) Necessity of electron transfer and a radical pair in the nitration of reactive aromatics. J Am Chem Soc 99:5516–5518. doi:10.1021/ja00458a065
12. Kochi JK (1992) Inner-sphere electron transfer in organic chemistry. Relevance to electrophilic aromatic nitration. Acc Chem Res 25:39–47. doi:10.1021/ar00013a006
13. Fukuzumi S, Kochi JK (1981) Electrophilic aromatic substitution. Charge-transfer excited states and the nature of the activated complex. J Am Chem Soc 103:7240–7252. doi:10.1021/ja00414a034
14. Peluso A, Del Re G (1996) On the occurrence of an electron-transfer step in aromatic nitration. J Phys Chem 100:5303–5309. doi:10.1021/jp9530156
15. Albunia AR, Borrelli R, Peluso A (2000) The occurrence of electron transfer in aromatic nitration: dynamical aspects. Theor Chem Acc 104:218–222. doi:10.1007/s002140000141
16. Esteves PM, De M, Carneiro JW, Cardoso SP et al (2003) Unified mechanistic concept of electrophilic aromatic nitration: convergence of computational results and experimental data. J Am Chem Soc 125: 4836–4849. doi:10.1021/ja021307w
17. De Queiroz JF, de Carneiro JWM, Sabino AA et al (2006) Electrophilic aromatic nitration: understanding its mechanism and substituent effects. J Org Chem 71:6192–6203. doi:10.1021/jo0609475
18. Chen L, Xiao H, Xiao J, Gong X (2003) DFT study on nitration mechanism of benzene with nitronium ion. J Phys Chem A 107: 11440–11444. doi:10.1021/jp030167p
19. Arrieta A, Cossıo FP (2007) Loss of aromaticity and π-electron delocalization in the first step of the electrophilic aromatic nitration of benzene, phenol and benzonitrile. J Mol Struct THEOCHEM 811: 19–26. doi:10.1016/j.theochem.2007.03.007
20. Wheeler SE, Houk KN (2009) Substituent effects in cation/pi interactions and electrostatic potentials above the centers of substituted benzenes are due primarily to through-space effects of the substituents. J Am Chem Soc 131:3126–3127. doi:10.1021/ja809097r

21. Koleva G, Galabov B, Wu JI et al (2009) Electrophile affinity: a reactivity measure for aromatic substitution. J Am Chem Soc 131: 14722–14727. doi:10.1021/ja902194y
22. Xu XF, Zilberg S, Haas Y (2010) Electrophilic aromatic substitution: the role of electronically excited states. J Phys Chem A 114:4924–4933. doi:10.1021/jp911250g
23. Hadzic M, Braïda B, Volatron F (2011) Wheland intermediates: an ab initio valence bond study. Org Lett 13:1960–1963. doi:10.1021/ol200327s
24. Schmitt RJ, Buttrill SE, Ross DS (1984) Gas-phase ion-molecule nitration chemistry: the nitration of aromatic radical cations by nitrogen dioxide. J Am Chem Soc 106:926–930. doi:10.1021/ja00316a017
25. Aschi M, Attina M, Cacace F, Ricci A (1994) Experimental study on the mechanism of gas-phase aromatic nitration by protonated methyl nitrate. J Am Chem Soc 116:9535–9542. doi:10.1021/ja00100a018
26. Attinà M, Cacace F, Speranza M (1992) FT-ICR studies of gas-phase ionic nitration of benzene: the role of electron- and proton-transfer processes. Int J Mass Spectrom Ion Proc 117:37–46. doi:10.1016/0168-1176(92)80084-E
27. Rocha CMR, Pereira DH, Morgon NH, Custodio R (2013) Assessment of G3(MP2)//B3 theory including a pseudopotential for molecules containing first-, second-, and third-row representative elements. J Chem Phys 139:184108. doi:10.1063/1.4826519
28. Curtiss LA, Redfern PC, Raghavachari K (2005) Assessment of Gaussian-3 and density-functional theories on the G3/05 test set of experimental energies. J Chem Phys 123:124107. doi:10.1063/1.2039080
29. Curtiss LA, Redfern PC, Raghavachari K et al (1999) Gaussian-3 theory using reduced Møller–Plesset order. J Chem Phys 110:4703. doi:10.1063/1.478385
30. Baboul AG, Curtiss LA, Redfern PC, Raghavachari K (1999) Gaussian-3 theory using density functional geometries and zero-point energies. J Chem Phys 110:7650. doi:10.1063/1.478676
31. Wang X, Lau K-C (2012) Theoretical investigations on charge-transfer properties of novel high mobility n-channel organic semiconductors—diazapentacene derivatives. J Phys Chem C 116: 22749–22758. doi:10.1021/jp309226z
32. Silva ALR, Cimas Á, Vale N et al (2013) Experimental and computational study of the energetics of hydantoin and 2-thiohydantoin. J Chem Thermodyn 58:158–165. doi:10.1016/j.jct.2012.10.010
33. Gao A, Liang X, Li L, Cui J (2013) A Gaussian-3 theoretical study of the alkylthio radicals and their anions: structures, thermochemistry, and electron affinities. J Mol Model 19:3225–3231. doi:10.1007/s00894-013-1855-3
34. Paine SW, Salam A (2013) Computational study of tautomerism and aromaticity in mono- and dithio-substituted tropolone. Int J Quantum Chem 113:1245–1252. doi:10.1002/qua.24268
35. Ducati LC, Custodio R, Rittner R (2010) Exploring the G3 method in the study of rotational barrier of some simple molecules. Int J Quantum Chem 110:2006–2014. doi:10.1002/qua.22585
36. Pereira DH, Ducati LC, Rittner R, Custodio R (2014) A study of the rotational barriers for some organic compounds using the G3 and G3CEP theories. J Mol Model 20:2199. doi:10.1007/s00894-014-2199-3
37. Kovacevic G, Sabljic A (2013) Theoretical study on the mechanism and kinetics of addition of hydroxyl radicals to fluorobenzene. J Comput Chem 34:646. doi:10.1002/jcc.23175
38. Mora JR, Lezama J, Berroteran N et al (2012) Density functional theory and ab initio study on the reaction mechanisms of the homogeneous, unimolecular elimination kinetics of selected 1-chloroalkenes in the gas phase. Int J Quantum Chem 112:3729. doi:10.1002/qua.24175
39. Ali MA, Rajakumar B (2010) Kinetics of OH radical reaction with CF_3CHFCH_2F (HFC-245eb) between 200 and 400 K: G3MP2, G3B3 and transition state theory calculations. J Mol Struct Theochem 949:73. doi:10.1016/j.theochem.2010.03.006
40. Stevens WJ, Basch H, Krauss M (1984) Compact effective potentials and efficient shared-exponent basis sets for the first- and second-row atoms. J Chem Phys 81:6026. doi:10.1063/1.447604
41. Stevens WJ, Krauss M, Basch H, Jasien PG (1992) Relativistic compact effective potentials and efficient, shared-exponent basis sets for the third-, fourth-, and fifth-row atoms. Can J Chem 70:612–630. doi:10.1139/v92-085
42. Pereira DH, Ramos AF, Morgon NH, Custodio RR (2011) Implementation of pseudopotential in the G3 theory for molecules containing first-, second-, and non-transition third-row atoms. J Chem Phys 135:034106. doi:10.1063/1.3609241
43. Pereira DH, Ramos AF, Morgon NH, Custodio RR (2011) Erratum: "Implementation of pseudopotential in the G3 theory for molecules containing first-, second-, and non-transition third-row atoms" [J. Chem. Phys. 135, 034106 (2011)]. J Chem Phys 135:219901. doi:10.1063/1.3666235
44. Curtiss LA, Redfern PC, Raghavachari K (2011) G n theory. Wiley Interdiscip Rev Comput Mol Sci 1:810. doi:10.1002/wcms.59
45. Fukui K (1981) The path of chemical reactions—the IRC approach. Acc Chem Res 14:363. doi:10.1021/ar00072a001
46. Šakić D, Vrček V (2012) Prereactive complexes in chlorination of benzene, triazine, and tetrazine: a quantum chemical study. J Phys Chem A 116:1298. doi:10.1021/jp210993k
47. Reed AE, Weinstock RB, Weinhold F (1985) Natural population analysis. J Chem Phys 83:735. doi:10.1063/1.449486
48. Glendening ED, Reed AE, Carpenter JE, Weinhold F (2009) program: NBO analysis, version 5.1
49. Frisch MJ, Trucks GW, Schlegel HB et al (2009) Gaussian 09. Gaussian, Inc., Wallingford
50. Herzberg G (1966) Molecular spectra and molecular structure: electronic spectra and electronic structure of polyatomic molecules. Van Nostrand, New York
51. Chen Z, Mo Y (2013) Electron transfer in electrophilic aromatic nitration and nitrosation: computational evidence for the Marcus inverted region. J Chem Theory Comput 9:4428. doi:10.1021/ct400618k
52. Vogel AI, Tatchell AR, Furnis BS et al (1989) Vogel's textbook of practical organic chemistry, 5th edn. Longman, London